*Cancer Research (Research Article)*

# Targeting FSTL1 prevents tumor bone metastasis and consequent immune dysfunction

**Running title:** Role of FSTL1 in cancer bone metastasis

Chie Kudo-Saito, Takafumi Fuwa, Kouichi Murakami and Yutaka Kawakami

Division of Cellular Signalling, Institute for Advanced Medical Research, Keio University School of Medicine, 35 Shinanomachi, Shinjuku-ku, Tokyo 160-8582, Japan

**Corresponding authors**

Chie Kudo-Saito (kudoc@a3.keio.jp) and Yutaka Kawakami (yutakawa@z5.keio.jp), Division of Cellular Signaling, Institute for Advanced Medical Research, Keio University School of Medicine, 35

Shinanomachi, Shinjuku-ku, Tokyo 160-8582, Japan. Phone: +81-3-5363-3778;

Fax: +81-3-5362-9259

Note: C.K.S. is the corresponding author to communicate with the Editorial office.

**Financial support**

This work was supported by Grant-in-Aid for Scientific Research from Japan Society for the Promotion of Science (19590405, 21590445, and 18591484), The Sagawa Foundation for Promotion of Cancer Research, and Keio Gijuku Academic Development Funds.

**Disclosure of potential conflicts of interest**

The authors have no conflicting financial interest to declare.

**Key words:** FSTL1; bone metastasis; $CD8^{low}$; mesenchymal stem; ALCAM

**The total number of words:** 4,958

**The number of figures:** 6

## Abstract

Bone metastasis greatly deteriorates the quality of life in cancer patients. While mechanisms have been widely investigated, the relationship between cancer bone metastasis and anti-tumor immunity in the host has been much less studied. Here we report a novel mechanism of bone metastasis mediated by FSTL1, a follistatin-like glycoprotein secreted by $Snail^+$ tumor cells, which metastasize frequently to bone. We found that FSTL1 plays a dual role in bone metastasis, in one way by mediating tumor cell invasion and bone tropism but also in a second way by expanding a population of pluripotent mesenchymal stem-like $CD45^-ALCAM^+$ cells derived from bone marrow. $CD45^-ALCAM^+$ cells induced bone metastasis de novo, but they also generated $CD8^{low}$ T cells with weak CTL activity in the periphery, which also promoted bone metastasis in an indirect manner. RNAi-mediated attenuation of FSTL1 in tumor cells prevented bone metastasis along with the parallel increase in $ALCAM^+$ cells and$CD8^{low}$ T cells. These effects were accompanied by heightened anti-tumor immune responses *in vitro* and *in vivo*. In clinical specimens of advanced breast cancer, $ALCAM^+$ cells increased with

FSTL1 positivity in tumor tissues, but not in adjacent normal tissues, consistent with a causal connection between these molecules. Our findings define FSTL1 as an attractive candidate therapeutic target to prevent or treat bone metastasis, which remains a major challenge in cancer patients.

## Introduction

Bone metastasis of tumor cells is frequently seen in cancer patients particularly with breast cancers and prostate cancers, and greatly deteriorates the quality of life in patients leading to poor prognosis (1). Chemokines and its receptors are one of the representative molecules regulating bone-tropism of tumor cells. For examples, $CXCR4^+$ tumor cells are attracted by CXCL12 secreted from stromal cells in bone marrow (BM) (2), and CXCL12 maintains proliferation and survival of the tumor cells (3). Bone-derived TGFβ and PDGF also promote tumor progression in BM (4). CCL2 is known as another chemokine critical for bone metastatic mechanism in various cancers (5, 6). The excess of tumor growth in BM results in disruption of skeletal integrity, and causes abnormal osteogenesis or osteolysis in cancer

patients (1). One of the most influential molecules is RANKL, which is highly expressed in normal mesenchymal cells including osteoblasts and stromal cells, and metastatic tumor cells undergoing epithelial-to-mesenchymal transition (EMT) (7).

A variety of therapeutics targeting these molecules has been developed for treating bone metastasis (4). However, their subjects are mostly post-metastasis events, but not pre-metastatic state. Elimination of the trigger for tumor seeding toward bone would be a higher priority of cancer therapy rather than treatment of tumor progression and osteo-imbalance in BM. Moreover, while bone metastasis mechanisms have been widely investigated, the relationship with anti-tumor immunity has been rarely explored, although BM is an essential organ for hematopoiesis and immune responses (8). We previously demonstrated a close relationship between cancer metastasis and immunosuppression focusing on an EMT-governing transcriptional factor Snail (9). Snail expression in tumor cells promotes both tumor metastasis and induction of immunoregulatory cells simultaneously. Some immunoregulatory members such as mesenchymal stem

cells (MSCs) (10) and myeloid-derived suppressor cells (MDSCs) (11) are originated from BM. To understand the interaction between bone metastasis and anti-tumor immunity may provide a new insight into bone metastasis mechanism. In this study, we attempted to elucidate a new mechanism of cancer bone metastasis from the immunological perspective.

## Materials and Methods

### Cell lines and mice

Murine melanoma B16-B10 cells were kindly provided by Cell Resource Center for Biomedical Research at Tohoku University in Japan. Human tumor cells including melanoma HS294T and pancreatic cancer Panc1 were purchased from ATCC, and were authenticated by short tandem repeat profiling. Some clones were transfected with plasmid vector pcDNA3.1 encoding murine or human *snail* gene as described before (9), and/or with lentiviral vector encoding GFP gene (Biogenova) for *in vivo* study. Tumor cells were cultured routinely in 10% FBS/DMEM (Invitrogen), and sometimes in 2% FBS/Opti-MEM (Invitrogen) for preparation of supernatant used

for assays. Female C57BL/6 and C57BL/6-CAG-EGFP mice (designated $EGFP^+$ mice) were purchased from SLC in Japan, and were maintained under pathogen-free conditions until use according to the protocols approved by the Animal Care and Use Committee at Keio University School of Medicine.

**Stimulation and characterization of bone marrow cells**

Bone marrow cells (BMCs) were stimulated with 25% tumor supernatant ($1x10^5$ cells/10ml/3 days, 0.22 μm filtration) or FSTL1 (5 ng/ml; Thermo Scientific) in 2% FBS/Opti-MEM for 7-10 days. $CD45^-$ BMCs were sorted from the culture using a MACS system with microbeads-conjugated mAb (Miltenyi Biotec), and were tested for MSC activities: differentiation activity into mesenchymal lineages using Mesenchymal Stem Cell Functional Identification Kit (R&D), self-renewal activity using 2% agarose medium, and immunoregulatory activity utilizing coculture with splenic T cells *in vitro*, and co-injection with tumors *in vivo*. The details were described in Supplementary data. For tracking $CD45^-ALCAM^+$ cell division, the sorted $CD45^-ALCAM^+$ cells were stained with red fluorescent dye PKH26 (Sigma) before assay.

**Functional analysis of tumor cells**

Tumor cells ($5x10^4$) were assessed for Matrigel-invasion (6 hrs) and chemotaxis (4 hrs) to CCL2 (R&D) or CXCL12 (R&D) using a transwell chamber with a membrane (pore size, 8 μm; BD Biosciences). FSTL1 in the supernatant fluids was measured using the ELISA kit (R&D) according to the manufacturer's instructions. For knockdown of *fstl1* or *snail* expression, the specific siRNAs or the scrambled oligonucleotides as a control (3 μg; Invitrogen) were complexed with jetPEI (PolyPlus), and were then transfected into tumor cells. The transfection efficacy was validated by RT-PCR 1-2 days after transfection. Several kinds of siRNAs targeting on a different sequence position of the genes were initially used, and a siRNA having the highest knockdown efficiency was mainly used. In a setting, tumor cells were stimulated with FSTL1 (5 ng/ml) in combination with/without CCL2 (5 ng/ml) for 3 days before assay.

**Flow cytometric analysis**

After Fc blocking, cells were stained with immunofluorescence (FITC, PE or CyChrome)-conjugated mAbs specific for mouse and/or human ALCAM (eBioscience), CCR2 (R&D), CCR5, CD146 (Abcam), CD271, CD45, CD8, CXCR4, DIP2A (SantaCruz), Foxp3, PDGFRa (R&D), RANK (R&D), RANKL (Avnova), tetramer for gp70 (a tumor antigen expressed in B16-F10; MBL), or the appropriate isotype control antibodies. The immunofluorescence-conjugated secondary antibodies were used if necessary. Antibodies except designated ones were purchased from BD Pharmingen. For intracellular staining, cells were treated with Cytofix/Cytoperm solution (BD). The immunofluorescence was analyzed and compared with the isotype controls by Cellquest software using a FACSCalibur cytometer (BD).

**Analysis of clinical tissues**

Paraffin-embedded tumor tissue sections obtained from Stage III breast cancer patients (n=26) and normal mammary tissue sections (n=6) were purchased (Human Cancer Tissue Array; MBL). To analyze mRNA expression, semi-quantitative RT-PCR was conducted using Ampdirect Plus (Shimadzu) and

the specific paired primers for human *fstl1*, *alcam* and *gapdh* (Supplementary data) as described before (9). The digital images of the bands were quantified using NIH ImageJ software, and the signal intensity was normalized to *gapdh* expression as a control (normal tissues, < 0.1). To analyze protein expression, immunohistochemical analysis was conducted with anti-FSTL1 mAb (Abcam) and anti-ALCAM mAb (LSBio) according to a general protocol (Supplementary data). As immunofluorescence intensity, pixel counts were automatically measured at two fields under the same DAPI level using a LSM700 Laser Scanning Microscope (Carl Zeiss), and the average data was plotted in graphs (FSTL1, < 66, ALCAM, < 233 in normal tissues).

**FSTL1 blocking therapy *in vivo***

To evaluate siRNA efficacy on tumor dissemination from the primary tumor site, and on tumor metastatic nodule formation, tumor cells were implanted into mice both s.c. ($5x10^5$) to prepare easy-accessible sites for siRNA injection, and i.v. ($1x10^5$) to make visible bone metastasis for a short term while F10-snail$^+$ tumor-implanted mice were living. Seven days later, PEI-complexed siRNAs (5 μg) were injected into

the s.c. tumors (n = 3-5/group), and the transfection efficacy was validated by RT-PCR or Western Blotting 1-2 days after injection. Tumor volume (0.5 x Length x Width$^2$, mm$^3$) was measured 1-2 times a week. Ten days after siRNA injection, the s.c. tumors, BM and spleens were analyzed by flow cytometry, and splenic CD8$^+$ T cells were tested for IFNγ production (24 hrs) and tumor-killing (4 hrs) as described before (9).

**Statistical analysis**

Significant differences (*P* value < 0.05) were evaluated using the unpaired two-tailed Student's *t* test. The significance was confirmed by the non-parametric Mann-Whitney U test using the cumulative data of the repeated experiments, when the number of n was small in one experiment. Mouse survival was analyzed by Kaplan-Meier method and ranked according to the Mantel-Cox log-rank test. Correlation between tumor bone metastasis and ALCAM$^+$ cells in mice, or between FSTL1 and ALCAM expressions in clinical tissues was evaluated by the nonparametric Spearman's rank test.

## Results

### Snail$^+$ tumor cells generate CD45$^-$ALCAM$^+$ mesenchymal stem cells in bone marrow

We previously established murine *snail*-transduced B16-F10 melanoma (designated F10-snail$^+$) having typical EMT features (9). When the F10-snail$^+$ tumor cells were implanted both s.c. and i.v. in C57BL/6 mice, tumor metastatic dissemination was more severely observed in various tissues such as lymph node, lung and BM, as compared to that of the mice implanted with B16-F10 tumors transduced with empty vectors (designated F10-mock) (Fig. S1A), although the s.c. tumor growth was slower than F10-mock growth as shown before (12). Particularly, there are many mice having black bones due to melanoma metastasis in the s.c./i.v. tumor model (41/48 = 85.4%; F10-mock, 1/12 = 8.3%), and the F10-snail$^+$ tumor cells spontaneously disseminated to bone rather than other tissues even after only s.c. implantation (Fig. S1B). These results suggest that Snail regulates bone tropism of B16-F10 tumor cells.

To examine how Snail$^+$ tumor cells would affect BM microenvironment, we stimulated BMCs with F10-snail$^+$ supernatant for 7-10 days. Many colony-forming cells were observed in the culture, and CD45$^-$ cells significantly increased as compared to the culture with F10-mock supernatant ($P$ = 0.0002; Fig. 1A). Indeed, in addition to tolerogenic DCs and Treg cells (but not MDSCs) reported before (9), CD45$^-$ cells also increased in the F10-snail$^+$-implanted mice (Fig. S1C). CD45$^-$ BMCs sorted from the culture with F10-snail$^+$ supernatant more frequently differentiated into mesenchymal lineages such as adipocytes and osteoblasts, and formed large sphere colonies as compared to the CD45$^-$ BMCs treated with none or F10-mock supernatant (Fig. 1B). This indicates that F10-snail$^+$-induced CD45$^-$ BMCs are MSCs having pluripotency and self-renewal activity. The Snail$^+$ tumor-induced MSCs (designated sMSCs) significantly suppressed splenic T-cell proliferation and cytokine production, indicating immunosuppressive activity ($P$ < 0.002 vs. F10-mock-treated BMCs; Fig. 1C). These results suggest that Snail$^+$ tumor cells expand MSCs in BM microenvironment.

The sMSCs highly expressed some MSC markers reported in human MSCs (13),

particularly ALCAM and CD146, as compared to the F10-mock-treated BMCs (Fig. 1D). However, the $CD45^{-}CD146^{+}$ subpopulation hardly differentiated into osteoblasts (Fig. S2). In contrast, the $CD45^{-}ALCAM^{+}$ subpopulation showed high differentiation activity (Fig. S2), proliferated in response to F10-$snail^{+}$ supernatant (Fig. 1E). ALCAM blocking with the specific mAb significantly suppressed the sMSC increase ($P = 0.001$; Fig. 1E), and significantly improved T-cell responses ($P < 0.002$; Fig. 1C). These data suggest that ALCAM is partly but critically responsible for the sMSC properties. ALCAM is a member of the immunoglobulin superfamily, and binds to CD6 expressed T cells with high affinity, and to ALCAM expressed various cells with low affinity (14). The ALCAM-ALCAM homophilic binding is strengthen by ALCAM clustering on the cell surface, and has been recently reported as a critical molecular interaction for proliferation and colonization of cancer stem cells (CSCs) (14). However, the functional role of ALCAM in MSCs remains unclear. Probably, sMSC expansion may be mediated by this homophilic interaction via ALCAM clustering, and T-cell suppression may be mediated by the heterophilic interaction.

**The sMSCs induce both tumor bone metastasis and immune dysfunction via generation of impaired CD8$^{low}$ T cells**

We next conducted in vivo study using GFP$^{+}$ tumor cells or EGFP$^{+}$ BMCs for cell tracking after injection in mice. When EGFP$^{+}$ sMSCs were i.v. injected in mice on day 7 after F10-mock s.c. implantation, the sMSCs mainly infiltrated in the tumors, and tumor growth was significantly promoted ($P$ = 0.002 vs. F10-mock-treated BMCs; Fig. 2A). To see how the infiltrating sMSCs would affect tumor microenvironment more clearly, the sMSCs were mixed with F10-mock tumor cells, and injected s.c. in mice. The tumors grew more aggressively ($P$ = 0.013 vs. F10-mock-treated BMCs), and CD8$^{low}$ T cells predominantly increased in the tumors (Fig. S3A). CD8$^{low}$ T cells also increased in spleen that was hypertrophic with abundant adipose tissues having increased CD45$^{-}$ cells including the injected sMSCs (Fig. 2B and Fig. S3B). The CD8$^{+/low}$ T cells sorted from spleen hardly produced IFNγ in response to a tumor antigen gp70 peptide, although weakly reacted to gp70 tetramer (Fig. 2B). It is inferred that such CTL dysfunction would be induced by the sMSCs infiltrating in spleen. In the sMSC-injected mice, tumor cells increased in BM (Fig. 2B and Fig. S3C), and the significant correlation was seen

between the number of tumor cells and ALCAM$^+$ cells in BM and the primary tumor site ($P < 0.05$; Fig. 2C). This suggests that sMSCs could induce bone metastasis *de novo* followed by further increase of ALCAM$^+$ sMSCs. Indeed, stimulation with the sMSC supernatant significantly enhanced tumor invasion *in vitro* ($P = 0.001$), and bone metastasis *in vivo* ($P = 0.006$; Fig. 2D). We found that the sMSCs significantly more produced CCL2 among soluble factors tested as EMT-inducible molecules ($P = 0.004$ vs. F10-mock-treated BMCs; Fig. 2D). CCL2 blocking with the specific mAb significantly inhibited the sMSC-induced tumor invasion *in vitro* ($P = 0.002$ vs. control IgG) and bone metastasis *in vivo* ($P = 0.006$; Fig. 2D). These results suggest that CCL2 is, at least in part, involved in the sMSC-induced bone metastasis mechanism. There may be a molecule that directly regulates this mechanism more significantly. The further study is needed. Tumor metastasis-promoting activity of MSCs has been already demonstrated using xenograft model implanted with human breast cancer cells and human BM-derived MSCs, and CCL5 has been demonstrated as a molecule essential for the activity (15). However, the sMSCs produced no CCL5, and no lung metastatic nodules were observed in the co-injected mice in our study (data not shown).

**FSTL1 is a key molecule governing Snail-induced bone metastasis**

To identify the specific molecule regulating the Snail-induced bone metastasis, we reviewed literature focusing on molecules that associate with “bone”-related diseases such as arthritis, leukemia and osteosarcoma, and about 20 candidates were chosen for analysis of mRNA and protein expressions. FSTL1 was the molecule that significantly and widely upregulated in murine and human Snail$^+$ tumor cells (Fig. 3A and Fig. S4). FSTL1 is a follistatin-like glycoprotein that binds to DIP2A receptor (16, 17). FSTL1 is originally known to regulate organ tissue formation in embryos (18), and its increase has been reported in some diseases such as rheumatoid arthritis (19, 20) and osteosarcoma (21). However, the functional role in cancer and metastasis has never been demonstrated.

Transfection with *fstl1*-specific siRNAs into Snail$^+$ tumor cells significantly inhibited tumor invasion ($P < 0.004$), bone metastasis-associated molecule expressions such as CCR2 and CXCR4, and migration to the ligand such as CCL2 and CXCL12 (Fig. 3C and Fig. S5), in addition to the typical reversal changes of EMT (for example, increased adhesion, and decreased CD44 expression (data not shown). When

Snail$^{-/low}$ tumor cells were stimulated with FSTL1, these molecular expressions and tumor invasion were significantly enhanced ($P < 0.002$; Fig. 3D). This suggests that FSTL1 is a critical effector molecule for the high metastatic activity of Snail$^{+}$ tumor cells. CCL2 combination synergistically elevated CXCR4 and RANK expressions (Fig. 3D). It is inferred that CCL2 produced from the sMSCs and Snail$^{+}$ tumor cells (12) may collaborate for promotion of bone metastasis. More interestingly, CD8$^{low}$ T-cell-inducible sMSC-like cells increased when BMCs were stimulated with FSTL1 (Fig. 4). The sMSCs highly expressed DIP2A (Fig. 1D). These results suggest that FSTL1 is responsible for both tumor metastasis and immune dysfunction in cancer bone metastasis mechanism.

We validated the FSTL1 effect in human system. When human PBMCs were stimulated with FSTL1 for 7 days, CD45$^{-/low}$ALCAM$^{+}$ cells increased in the culture (Fig. S5D). When the sorted CD45$^{-/low}$ALCAM$^{+}$ cells were co-injected s.c. with human breast cancer MDA231 cells into in immunodeficient mice, tumor bone metastasis was caused (Fig. S5D), although the s.c. tumor growth was not enhanced (data not shown). ALCAM$^{+}$ MSC increase may be more closely

associated with tumor bone metastasis rather than T-cell impairment, and T-cell impairment may be required for further tumor progression. We analyzed tumor tissues of Stage III breast cancer patients possibly having bone metastasis and deteriorated immunity immunohistologically, since bone metastasis frequently occurs in breast cancer patients (1). Colonizing ALCAM$^+$ cells significantly increased in FSTL1$^+$ tumor tissues, but not normal tissues, and the significant correlation between FSTL1 and ALCAM increase was seen ($P < 0.01$; Fig. 5). This suggests a causal connection between these molecules in tumor microenvironment. To clarify the usefulness of these molecules for diagnosis and prognosis of cancer patients, the further studies are needed using other cancers and BM samples of patients at varying stages.

**FSTL1 blockade inhibits bone metastasis and immune dysfunction *in vivo***

To evaluated the anti-tumor efficacy of FSTL1 blocking, F10-snail$^+$ cells were implanted both s.c. and i.v. in mice, and PEI-complexed siRNA-*fstl1* was injected into the s.c. tumors on day 7. Tumor growth ($P = 0.012$; Fig. 6A) and bone metastasis ($P = 0.0002$; Fig. 6B) was significantly suppressed, and the mouse

survival ($P < 0.0001$; Fig. 6C) was significantly prolonged as compared to those of the control siRNA group. In the siRNA-*fstl1*-injected mice, increase of $ALCAM^+$ cells (Fig. 6D) and $CD8^{low}$ T cells (Fig. 6E) was not seen, and tumor-specific $CD8^+$ T-cell responses were significantly elevated ($P < 0.002$; Fig. 6F). The siRNA-*fstl1* efficacy was higher than that of siRNA-*snail*, particularly on induction of $ALCAM^+$ sMSCs and $CD8^{low}$ T cells. These results suggest that FSTL1 knockdown prevent not only tumor metastasis, but also immune dysfunction through $ALCAM^+$ sMSC decrease, and therefore anti-tumor CTLs are induced rightly for eliminating tumor cells from the mice. FSTL1 blockade may be a promising strategy for treating cancer bone metastasis of patients.

## DISCUSSION

The relationship between cancer bone metastasis and anti-tumor immunity in the host has been rarely investigated. This study revealed a novel mechanism, which is governed by FSTL1 produced from $Snail^+$ tumor cells undergoing EMT. FSTL1 plays a dual role in cancer bone metastasis, in one way by mediating tumor

invasion and bone tropism, and in a second way by expanding pluripotent and multifunctional $CD45^{-}ALCAM^{+}$ MSC-like cells, named as sMSCs. The sMSCs are possibly derived from BMCs, and disseminate all over the body. Tumor-infiltrating sMSCs induce bone metastasis *de novo* followed by further increase of sMSCs in BM. The sMSCs are able to generate $CD8^{low}$ T cells with almost no CTL activities, leading to dysfunction of anti-tumor immune responses. The number of $ALCAM^{+}$ cells is correlated with the amount of tumor bone metastasis in a murine model, and $ALCAM^{+}$ cells correlatively increase in $FSTL1^{+}$ tumor tissues of advanced breast cancer patients, who may have bone metastasis and deteriorated immune status frequently. FSTL1 blocking *in vivo* significantly prevents both tumor bone metastasis and increase of $ALCAM^{+}$ cells and $CD8^{low}$ T cells, and significantly ameliorates induction of anti-tumor immune responses in the host. Thus, FSTL1 is a prominent trigger to drive cancer bone metastasis accompanied by immune dysfunction (Fig. S6).

Although FSTL1 increase in some tumor cell lines has been shown previously (21), the functional role has not been investigated in cancer. We clarified that FSTL1

critically regulates cancer bone metastasis. FSTL1 would be a potential target for treating bone metastasis in patients. FSTL1 combination with other established drugs would treat bone metastasis more effectively. It has been shown that BM-derived MSCs express FSTL1 (22). Also, some $ALCAM^+$ cells expressed FSTL1 in the clinical tumor tissues tested in our study. FSTL1 may be a useful marker for “mesenchymal” cells regardless of normal or cancerous cells.

CCL2 is one of the molecules involved in bone metastatic mechanism (5, 6). Surely, CCL2 significantly increased in $Snail^+$ tumor cells, and siRNA-*ccl2* injection significantly suppressed $Snail^+$ tumor growth and dissemination/metastasis as shown before (12). However, the siRNA-*ccl2* injection hardly suppressed $CD45^-ALCAM^+$ MSC expansion in the treated mice, and the siRNA-*ccl2* efficacy was lower than siRNA-*fstl1* efficacy on bone metastasis and $CD8^{low}$ T-cell induction (data not shown). This suggest that FSTL1 blocking is more effective in treating cancer, at least in association with bone metastasis, since $CD45^-ALCAM^+$ MSCs are the upstream cells capable of inducing various immunoregulatory cells such as tolerogenic DCs and Treg cells.

In contrast to human MSCs, murine MSCs have not been fully characterized yet. As murine MSCs, non-stimulated adherent $CD45^-$ BMCs obtained from naive mice are generally used after long-term culture to obtain the adequate number of MSCs (13). However, we found that murine MSCs, which were phenotypically and functionally similar to human MSCs (13), increased in mice having $Snail^+FSTL1^+$ tumors *in vivo*, and are expanded by tumor-derived FSTL1 for a short term *in vitro*. FSTL1 was selectively expressed in tumor cells of patients, and stimulation with FSTL1 induced sMSC-like $CD45^{-/low}ALCAM^+$ cells in human PBMCs. A specific circumstance under cancer would lead to the finding of the sMSCs.

Some reports have shown induction of immunosuppressive T cells by MSCs. However, CD8 reduction was not shown in the report of $Foxp3^+$ Treg induction (23), and Foxp3 expression was not shown in the report of $CD4^{low}$ or $CD8^{low}$ T-cell induction (24). Our study additionally demonstrated that the sMSCs generate $CD8^{low}$ T cells partly including $CD8^{low}Foxp3^+$ cells. CD8 reduction in T cells may be mediated by zinc-finger protein MAZR (25) and/or cKrox (26), which are negative

regulators of CD8 expression in thymocyte lineage differentiation. The signalling pathway of ALCAM, which is possibly required for $CD8^{low}$ T-cell induction, may be of interest for elucidation of this mechanism.

Taken together, FSTL1 is a critical determinant governing cancer bone metastasis accompanied by immune dysfunction, and may be an attractive target for treating cancer via reprogramming of anti-tumor immune responses in patients.

**Author contributions**

C. Kudo-Saito designed and conducted the research, and wrote the manuscript; T. Fuwa and K. Murakami conducted *in vitro* experiments to analyze the molecular mechanism; and Y. Kawakami assisted with critical discussion.

## References

1. Weilbaecher KN, Guise TA, and McCauley LK. Cancer to bone: a fatal attraction. Nat Rev Cancer 2011;11:411-25.

2. Wang J, Loberg R, and Taichman RS. The pivotal role of CXCL12 (SDF-1)/CXCR4 axis in bone metastasis. Cancer Metastasis Rev 2006;25:573-87.

3. Burger JA, and Kipps TJ. CXCR4: a key receptor in the crosstalk between tumor cells and their microenvironment. Blood 2006;107:1761-7.

4. Lipton A. Future treatment of bone metastases. Clin Cancer Res 2006;12:6305s-08s.

5. Lu Y, Chen Q, Corey E, Xie W, Fan J, Mizokami A, et al. Activation of MCP-1/CCR2 axis promotes prostate cancer growth in bone. Clin Exp Metastasis 2009;26:161-9.

6. Cai Z, Chen Q, Chen J, Lu Y, Xiao G, Wu Z, et al. Monocyte chemotactic protein 1 promotes lung cancer-induced bone resorptive lesions in vivo. Neoplasia 2009;11:228-36.

7. Zhau HE, Odero-Marah V, Lue HW, Nomura T, Wang R, Chu G, et al. Epithelial to mesenchymal transition (EMT) in human prostate cancer: lessons learned from ARCaP model. Clin Exp Metastasis 2008;25:601-10.

8. Feuerer M, Beckhove P, Garbi N, Mahnke Y, Limmer A, Hommel M, et al. Bone marrow as a priming site for T-cell responses to blood-borne antigen. Nat Med 2003;9:1151-7.

9. Kudo-Saito C, Shirako H, Takeuchi T, and Kawakami Y. Cancer metastasis is accelerated through immunosuppression during Snail-induced EMT of cancer cells. Cancer Cell 2009;15:195-206.

10. Uccelli A, Moretta L, and Pistoia V. Mesenchymal stem cells in health and disease. Nat Rev Immunol 2008;8:726-36.

11. Bianchi G, Borgonovo G, Pistoia V, and Raffaghello L. Immunosuppressive cells and tumour microenvironment: focus on mesenchymal stem cells and myeloid derived suppressor cells. Histol Histopathol 2011;26:941-51.

12. Kudo-Saito C, Shirako H, Ohike M, Tsukamoto N, and Kawakami Y. CCL2 is critical for immunosuppression to promote cancer metastasis. Clin Exp Metastasis 2013;30:393-405.

13. Beyer Nardi N, and da Silva Meirelles L. Mesenchymal stem cells: isolation, in vitro expansion and characterization. Handb Exp Pharmacol 2006:249-82.

14. Weidle UH, Eggle D, Klostermann S, and Swart GW. ALCAM/CD166: cancer-related issues. Cancer Genomics Proteomics 2010;7:231-43.

15. Karnoub AE, Dash AB, Vo AP, Sullivan A, Brooks MW, Bell GW, et al. Mesenchymal stem cells within tumour stroma promote breast cancer metastasis. Nature 2007;449:557-63.

16. Tanaka M, Murakami K, Ozaki S, Imura Y, Tong XP, Watanabe T, et al. DIP2 disco-interacting protein 2 homolog A (Drosophila) is a candidate receptor for follistatin-related protein/follistatin-like 1--analysis of their binding with TGF-beta superfamily proteins. Febs J 2010;277:4278-89.

17. Ouchi N, Asaumi Y, Ohashi K, Higuchi A, Sono-Romanelli S, Oshima Y, et al. DIP2A functions as a FSTL1 receptor. J Biol Chem 2010;285:7127-34.

18. Adams D, Larman B, and Oxburgh L. Developmental expression of mouse Follistatin-like 1 (Fstl1): Dynamic regulation during organogenesis of the kidney and lung. Gene Expr Patterns 2007;7:491-500.

19. Miyamae T, Marinov AD, Sowders D, Wilson DC, Devlin J, Boudreau R, et al. Follistatin-like protein-1 is a novel proinflammatory molecule. J Immunol 2006;177:4758-62.

20. Li D, Wang Y, Xu N, Wei Q, Wu M, Li X, et al. Follistatin-like protein 1 is elevated in systemic autoimmune diseases and correlated with disease activity in patients with rheumatoid arthritis. Arthritis Res Ther 2011;13:R17.

21. Hambrock HO, Kaufmann B, Muller S, Hanisch FG, Nose K, Paulsson M, et al. Structural characterization of TSC-36/Flik: analysis of two charge isoforms. J Biol Chem 2004;279:11727-35.

22. Genovese JA, Spadaccio C, Rivello HG, Toyoda Y, and Patel AN. Electrostimulated bone marrow human mesenchymal stem cells produce follistatin. Cytotherapy 2009;11:448-56.

23. Prevosto C, Zancolli M, Canevali P, Zocchi MR, and Poggi A. Generation of CD4+ or CD8+ regulatory T cells upon mesenchymal stem cell-lymphocyte interaction. Haematologica 2007;92:881-8.

24. Giuliani M, Fleury M, Vernochet A, Ketroussi F, Clay D, Azzarone B, et al. Long-lasting inhibitory effects of fetal liver mesenchymal stem cells on T-lymphocyte proliferation. PLoS One 2011;6:e19988.

25. Bilic I, Koesters C, Unger B, Sekimata M, Hertweck A, Maschek R, et al. Negative regulation of CD8 expression via Cd8 enhancer-mediated recruitment of the zinc finger protein MAZR. Nat Immunol 2006;7:392-400.

26. Jenkinson SR, Intlekofer AM, Sun G, Feigenbaum L, Reiner SL, and Bosselut R. Expression of the transcription factor cKrox in peripheral CD8 T cells reveals substantial postthymic plasticity in CD4-CD8 lineage differentiation. J Exp Med 2007;204:267-72.

## Figure Legends

**Figure 1. Snail$^+$ tumor cells induce CD45$^-$ALCAM$^+$ mesenchymal stem cells.**

BMCs were stimulated with supernatant of murine melanoma B16-F10 cells transfected with *snail* (designated F10-snail$^+$) or empty vector (designated F10-mock) for 7-10 days, and were analyzed for CD45$^-$ cells by flow cytometry (A). The cultured BMCs were shown in photo (scale bar = 50 μm). The number of CD45$^-$ BMCs in the culture was calculated (n=3, mean ± SD). The sorted CD45$^-$ BMCs were tested for differentiation into FABP4$^+$ adipocytes and Osteocalcin$^+$ osteoblasts (B), sphere formation (B), and immunosuppression (C). Scale bar = 200 μm. In C, the sorted CD45$^-$ BMCs were added to the T-cell proliferation system (1:10) with/without anti-ALCAM neutralizing mAb (5 days), and cytokines in the supernatant fluids were measured (n=3, mean ± SD). The CD45$^-$ BMCs were further analyzed for MSC marker expression by flow cytometry (thin lines, F10-mock-treated BMCs; thick lines, F10-snail$^+$-treated BMCs). PKH26-labeled CD45$^-$ALCAM$^+$ BMCs proliferated in response to F10-snail$^+$ supernatant, and the CD45$^-$ BMC increase was suppressed by anti-ALCAM neutralizing mAb (E). The

number of BMCs was calculated (n=3, mean ± SD). *$P < 0.002$ vs. F10-mock-treated BMCs. □□$P < 0.002$ vs. control IgG. Data in each panel are representative of three independent experiments.

**Figure 2. The Snail$^{+}$ tumor-induced MSCs induce both tumor progression and immune dysfunction via generation of impaired CD8$^{low}$ T cells.**

A, Mice were s.c. implanted with F10-mock tumor cells ($3x10^5$), and 7 days later, received i.v. injection with the 10-day-cultured CD45$^{-}$ BMCs ($3x10^5$) obtained from EGFP$^{+}$ mice (n=5 per experiment). Eighteen days later, tumor size was measured (mean ± SD), and tumor-infiltrating cells were analyzed for the injected EGFP$^{+}$ BMCs by flow cytometry. B, Mice were s.c. injected with the mixture of CD45$^{-}$ BMCs ($3x10^5$) and GFP$^{+}$ F10-mock tumor cells ($3x10^5$). Twenty-five days later, tumor size was measured (n=5, mean ± SD), and BMCs and SPCs were analyzed for the injected GFP$^{+}$ tumor cells or CD8$^{+}$gp70-tetramer$^{+}$ T cells by flow cytometry (n=3, pooled). CD8$^{low}$ T cells was shown at the upper-left in dot plot. IFNγ-producible activity of the splenic CD8$^{+/low}$ T cells was evaluated (n=3, mean ± SD). The s.c. tumors and BM tissues were harvested from the mice, and were

immunocytochemically analyzed for ALCAM$^+$ cells and GFP$^+$ tumor cells (C). The number of positive cells was microscopically counted at triplicate sites, and the average data was plotted in graphs (n=15). Scale bar = 50 μm. D, Some EMT inducers in the CD45$^-$ BMC-cultured supernatant (7 days) were measured (n=3, mean ± SD). To evaluate the EMT-inducible activity, F10-mock tumor cells were stimulated with supernatant of F10-snail$^+$-treated BMCs (sMSCs) with/without anti-TNFα or anti-CCL2 neutralizing mAb for 3 days, and were tested by matrigel-invasion assay (n=3, mean ± SD). Also, mAbs were intratumorally injected into the 7-day-s.c. tumors mixed with sMSCs ($3x10^5$) and GFP$^+$ F10-mock cells ($3x10^5$), and 18 days later, the number of GFP$^+$ tumor cells in BM was microscopically counted (n=5, mean ± SD). *$P < 0.01$ vs. BMCs treated with none or F10-mock. □□$P < 0.01$ vs. control IgG. Data in each panel are representative of three independent experiments.

**Figure 3. FSTL1 regulates bone tropism of Snail$^+$ tumor cells.**

A, Increase of FSTL1 in the 3-day-cultured supernatant of *snail*-transfected tumor cells (murine melanoma B16-F10, human melanoma HS294T, and human

pancreatic cancer Panc1) (n=3, mean ± SD). *$P$ < 0.001 vs. mock. B, Transfection with siRNAs specific for *fstl1* or *snail* into F10-snail$^+$ cells inhibited FSTL1 production. *$P$ < 0.001 vs. control siRNA. C, The siRNA-*fstl1* transfection also inhibited cell invasion (n=3, mean ± SD), bone metastasis-associated molecule expressions, and chemotactic activity to the ligands. *$P$ < 0.03 vs. control siRNA. D, FSTL1 stimulation enhanced tumor invasion (n=3, mean ± SD), and bone metastasis-associated molecule expressions of F10-mock cells (n=3, mean ± SD). *$P$ < 0.002 vs. none, □□$P$ < 0.01 vs. FSTL1 alone. Data in each panel are representative of three independent experiments.

**Figure 4. FSTL1 generates the CD8$^{low}$ T-cell-inducible sMSCs.**

BMCs were treated with stimulants for 10 days, and were analyzed by flow cytometry (A). The sorted CD45$^-$ BMCs treated with none (MSC), F10-snail$^+$ supernatant (sMSCs) or FSTL1 (fMSCs) were tested for differentiation into FABP4$^+$ adipocytes and Osteocalcin$^+$ osteoblasts (B), sphere formation (B), and immunosuppression (C). Scale bar = 200 μm. In C, the CD45$^-$ BMCs were added to the CD8$^+$ T-cell proliferation system (1:10) with/without anti-ALCAM neutralizing

mAb (5 days), and IFNγ in the supernatant fluids were measured (n=3, mean ± SD; *$P < 0.003$ vs. MSC). CD8 expression of the cocultured $CD8^+$ T cells was also analyzed by flow cytometry. The $CD45^-$ BMCs ($3x10^5$) were mixed with $GFP^+$ F10-mock cells ($3x10^5$), and were s.c. injected into mice. Four weeks later, the BMCs of the mice were immunocytochemically analyzed for $ALCAM^+$ cells and $GFP^+$ tumor cells (D). Scale bar = 50 μm. Data in each panel are representative of three independent experiments.

**Figure 5. $ALCAM^+$ cells correlatively increase in $FSTL1^+$ tumor tissues of advanced breast cancer patients.**

Tumor tissues obtained from patients with Stage III breast cancers (n=26) and normal mammary tissues (n=6) were analyzed by semi-quantitative RT-PCR (A), and immunohistochemically using anti-FSTL1 mAb and anti-ALCAM mAb (B, C). Bar graph indicates mean ± SD. C, Representative photos (scale bar = 100 μm). The partial enlarged photo shows a tumor site positive for FSTL1, and colonizing cells strongly positive for ALCAM. ALCAM staining was only faintly seen in stroma.

**Figure 6. FSTL1 blocking inhibits tumor bone metastasis and anti-tumor immune dysfunction *in vivo*.**

F10-snail$^+$ or F10-mock tumor cells were implanted both s.c. ($5x10^5$) and i.v. ($1x10^5$) into mice, and 7 days later, siRNA was injected into the s.c. tumors (n=5-10 per experiment). Knockdown efficacy on day 2 was confirmed by western blotting (S, Snail; F, FSTL1; A, Actin; A). In the mice having F10-snail$^+$ tumors injected with siRNA-*fstl1* (closed triangles, siF) or siRNA-*snail* (closed squares, siS), the s.c. tumor growth (n=10, mean ± SD; A) and bone metastasis (n=9, mean ± SD; B) were suppressed, and the mouse survival was prolonged by (n=10; C). Open circles (M), F10-mock tumors. Closed circles (C), F10-snail$^+$ tumors injected with control siRNA. Ten days after siRNA injection, the s.c. tumors, BM and spleens of the mice were analyzed for ALCAM$^+$ cells as MSCs (n=6, mean ± SD; D). SPCs were further analyzed for CD8$^+$gp70-tetramer$^+$ T cells and CD8$^+$Foxp3$^+$ T cells by flow cytometry (E), and the sorted CD8$^+$ T cells were tested for F10-mock tumor-killing (ET ratio=50:1; n=3, mean ± SD; F) and IFNγ production (n=3, mean ± SD; F). *$P < 0.02$ vs. control siRNA. Data in each panel are representative of three independent experiments.

Author Manuscript Published OnlineFirst on August 21, 2013; DOI: 10.1158/0008-5472.CAN-13-1364
Author manuscripts have been peer reviewed and accepted for publication but have not yet been edited.



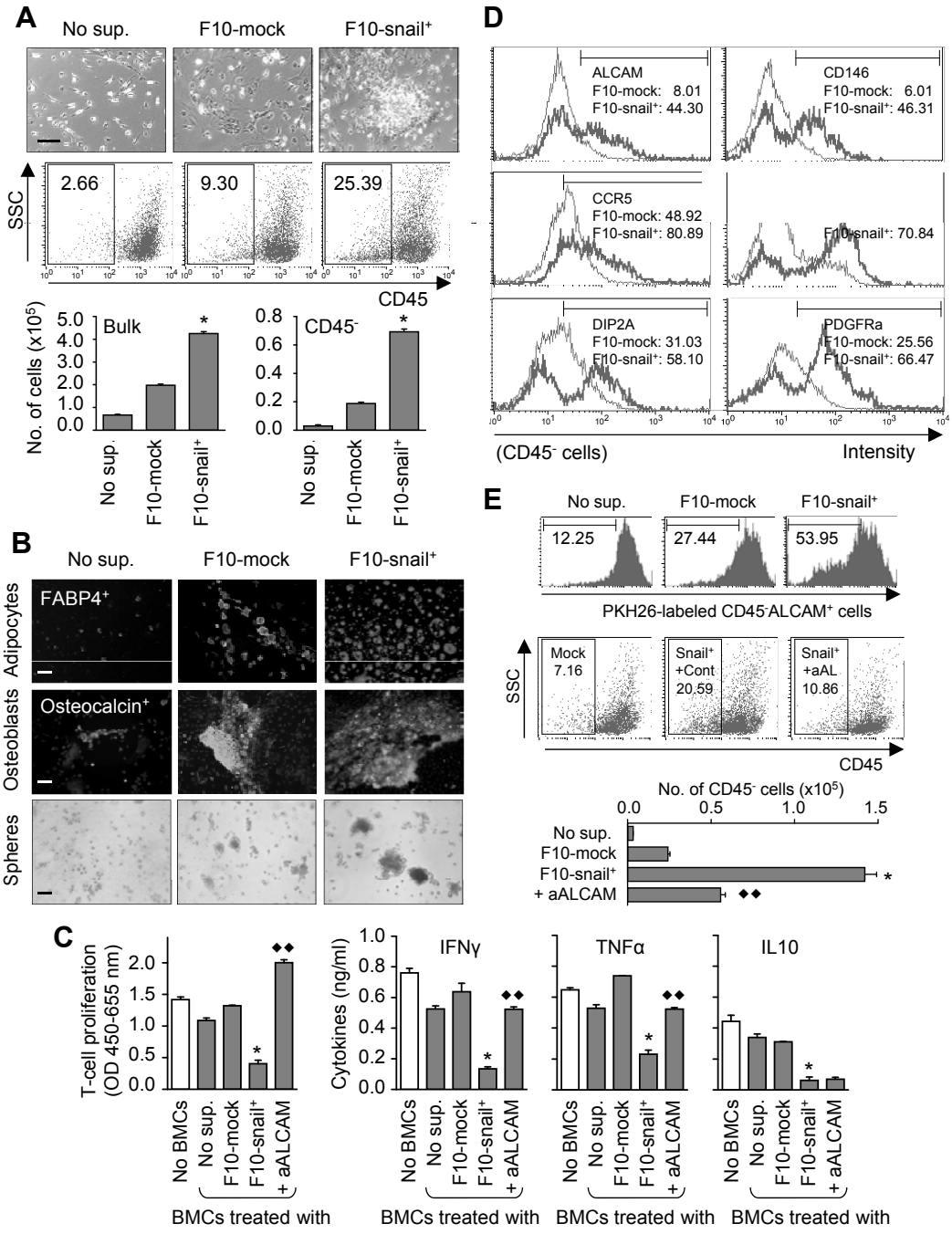

Author Manuscript Published OnlineFirst on August 21, 2013; DOI: 10.1158/0008-5472.CAN-13-1364
Author manuscripts have been peer reviewed and accepted for publication but have not yet been edited.



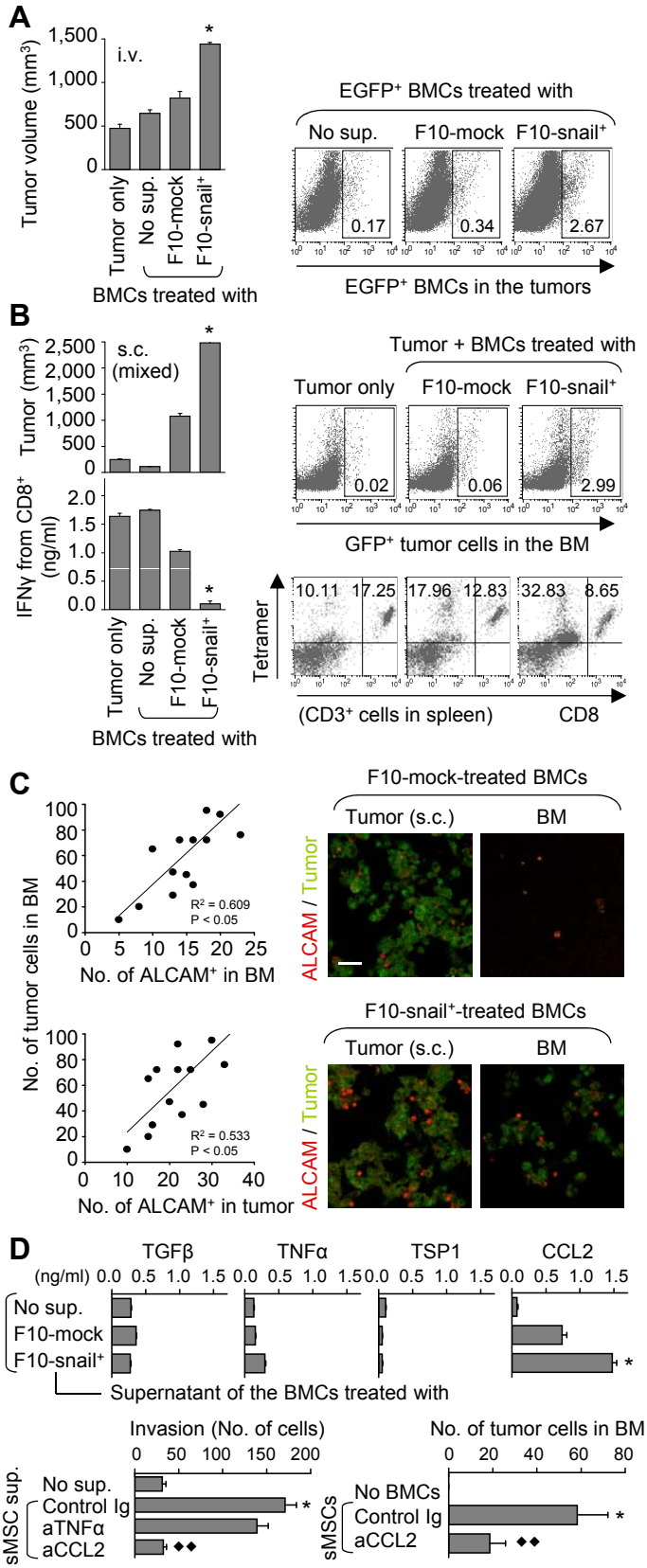

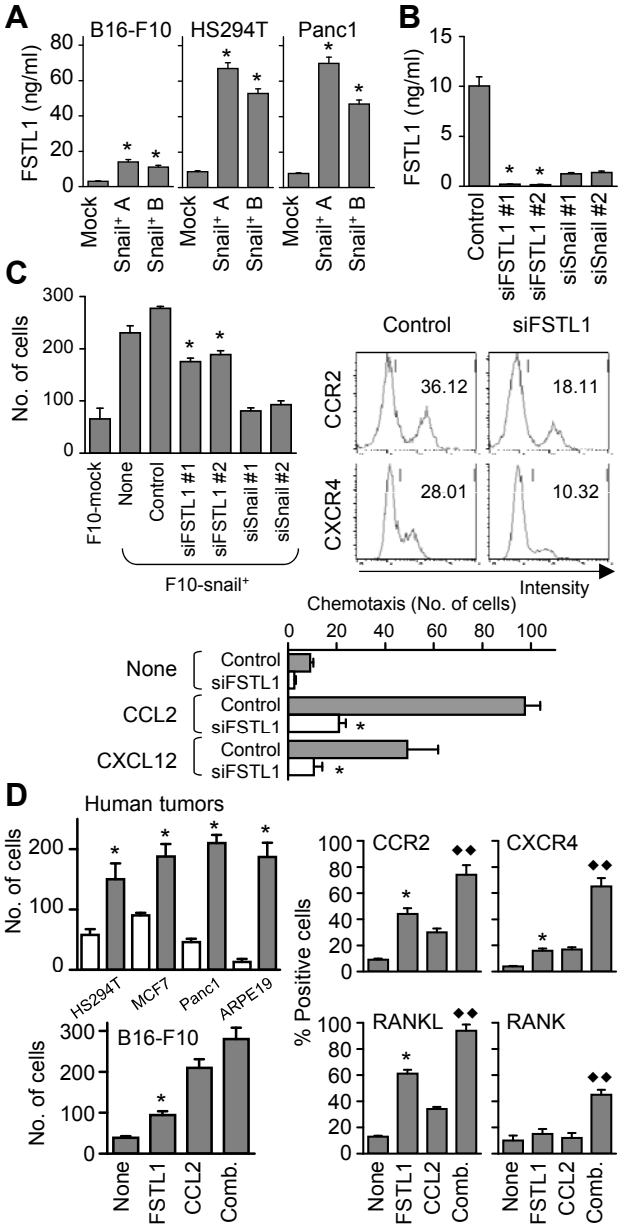

Author Manuscript Published OnlineFirst on August 21, 2013; DOI: 10.1158/0008-5472.CAN-13-1364
Author manuscripts have been peer reviewed and accepted for publication but have not yet been edited.

Kudo-Saito, et al.
Figure 4

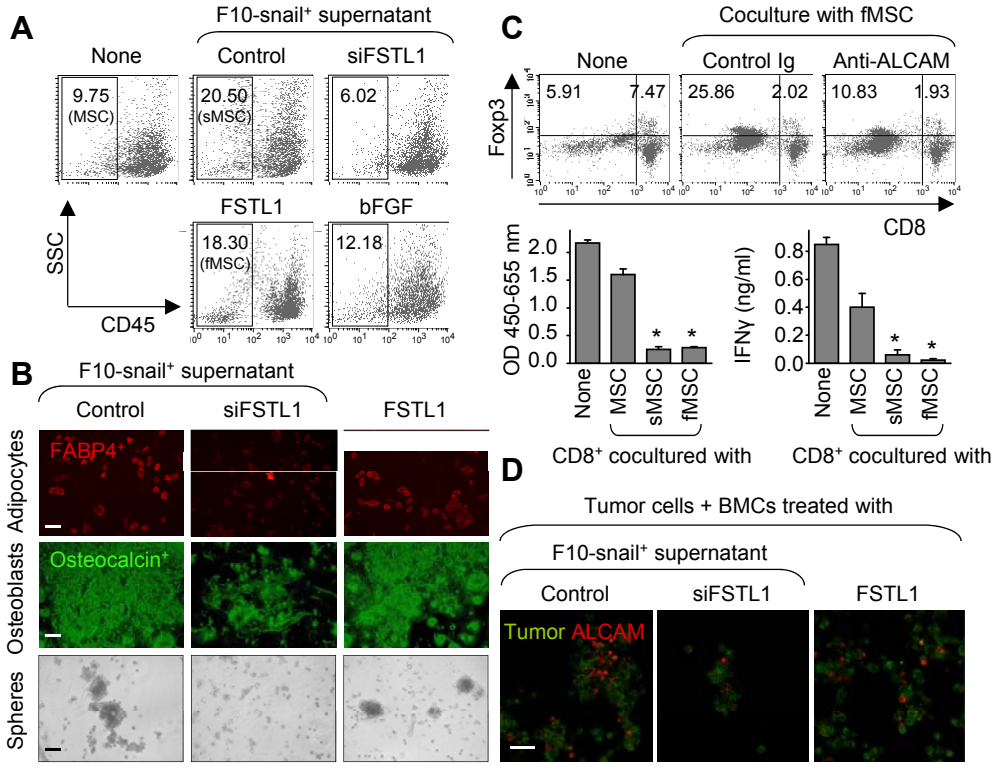

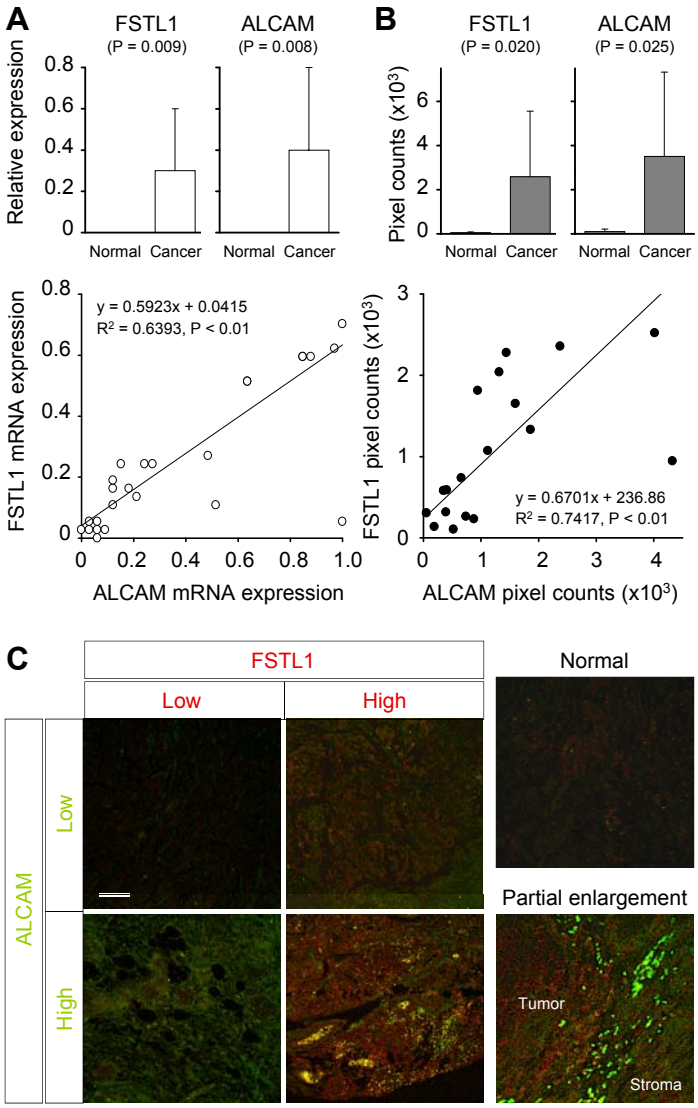

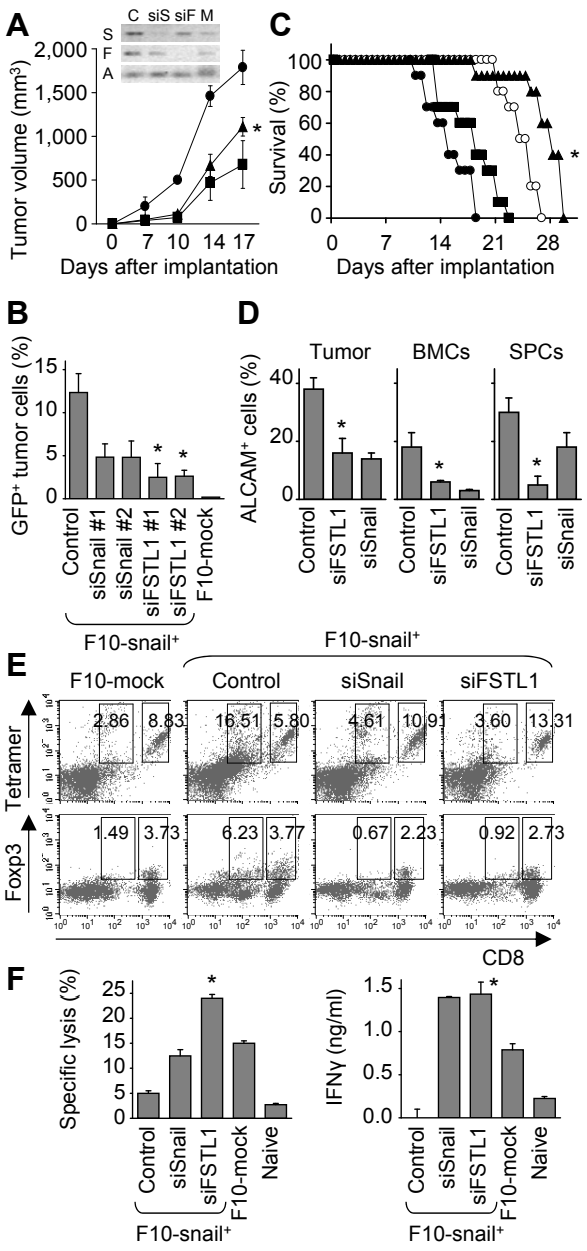

AACR American Association for Cancer Research

Cancer Research

The Journal of Cancer Research (1916–1930) | The American Journal of Cancer (1931–1940)

# Targeting FSTL1 prevents tumor bone metastasis and consequent immune dysfunction

Chie Kudo-Saito, Takafumi Fuwa, Kouichi Murakami, et al.

*Cancer Res* Published OnlineFirst August 21, 2013.